The Journal of Immunology

Regulatory and Helper Follicular T Cells and Antibody Avidity to Simian Immunodeficiency Virus Glycoprotein 120

Matthew J. Blackburn, Ma Zhong-Min, Francesca Caccuri, Katherine McKinnon, Luca Schifanella, Yongjun Guan, Giacomo Gorini, David Venzon, Claudio Fenizia, Nicolò Binello, Shari N. Gordon, Christopher J. Miller, Genoveffa Franchini and Monica Vaccari

J Immunol 2015; 195:3227-3236; Prepublished online 21 August 2015;
doi: 10.4049/jimmunol.1402699
http://www.jimmunol.org/content/195/7/3227

The Journal of Immunology is published twice each month by
The American Association of Immunologists, Inc.,
1451 Rockville Pike, Suite 650, Rockville, MD 20852

Print ISSN: 0022-1767 Online ISSN: 1550-6606.

Regulatory and Helper Follicular T Cells and Antibody Avidity to Simian Immunodeficiency Virus Glycoprotein 120

Matthew J. Blackburn,* Ma Zhong-Min,† Francesca Caccuri,*,[1] Katherine McKinnon,* Luca Schifanella,* Yongjun Guan,‡ Giacomo Gorini,* David Venzon,§ Claudio Fenizia,* Nicolò Binello,* Shari N. Gordon,* Christopher J. Miller,† Genoveffa Franchini,* and Monica Vaccari*

T follicular regulatory cells (T_{FR}) are a suppressive $CD4^+$ T cell subset that migrates to germinal centers (GC) during Ag presentation by upregulating the chemokine receptor CXCR5. In the GC, T_{FR} control T follicular helper cell (T_{FH}) expansion and modulate the development of high-affinity Ag-specific responses. In this study, we identified and characterized T_{FR} as $CXCR5^+CCR7^-$ "follicular" T regulatory cells in lymphoid tissues of healthy rhesus macaques, and we studied their dynamics throughout infection in a well-defined animal model of HIV pathogenesis. T_{FR} were infected by SIV_{mac251} and had comparable levels of SIV DNA to $CXCR5^-$ $CCR7^+$ "T zone" T regulatory cells and T_{FH}. Contrary to the SIV-associated T_{FH} expansion in the chronic phase of infection, we observed an apparent reduction of T_{FR} frequency in cell suspension, as well as a decrease of $CD3^+Foxp3^+$ cells in the GC of intact lymph nodes. T_{FR} frequency was inversely associated with the percentage of T_{FH} and, interestingly, with the avidity of the Abs that recognize the SIV gp120 envelope protein. Our findings show changes in the T_{FH}/T_{FR} ratio during chronic infection and suggest possible mechanisms for the unchecked expansion of T_{FH} cells in HIV/SIV infection. ***The Journal of Immunology*****, 2015, 195: 3227–3236.**

The generation of long-lived plasma cells and high-affinity Abs is largely dependent on T cell/B cell interaction in the B follicles of secondary lymphoid organs (1–3). Ag-activated B cells making contact with a specialized subset of $CD4^+$ T cells, called T follicular helper cells (T_{FH}), can enter the germinal centers (GC) to undergo somatic hypermutation and affinity maturation (4). T_{FH} home to B follicles and GC (5–9) by upregulating CXCR5 and downregulating CCR7 (5, 6, 10). T_{FH} express high levels of programmed death 1 (PD-1), ICOS, and Bcl-6, a master transcriptional regulator that orchestrates T_{FH} differentiation (11–13). In the GC, T_{FH} provide signals for B cell survival and differentiation (5, 10) via IL-21 production and CD40L expression, and they promote the generation of Abs with high affinity (11–16).

GC reactions are tightly regulated to prevent the emergence of B cell clones that are specific or cross-reactive against self-antigens, while selecting for high-affinity Abs to microbes (17, 18). The maintenance of the appropriate number of T_{FH} is crucial (19); the absence of T_{FH} has a negative impact in the generation of the GC (20, 21), whereas their excessive accumulation leads to increased GC reactions and the onset of some autoimmune diseases (4, 22–24).

$CD4^+$ T follicular regulatory cells (T_{FR}) contain T_{FH} numbers and, in doing so, they control the magnitude of GC responses (25, 26). Similarly to T_{FH}, T_{FR} migrate to the GC by expressing CXCR5 and downregulating CCR7 during T cell activation (6, 25, 27–29). T_{FR} differentiate from natural $CXCR5^-Foxp3^+CD25^+$ T regulatory cells (T_{REG}) and express high levels of the typical T_{REG} markers (i.e., Foxp3, CD25, CTLA-4) and T_{FH} canonical markers such as ICOS, PD-1, and Bcl-6 (25, 26). Whereas Bcl-6 is essential for CXCR5 expression on B cells and T_{FH} and for their localization to the GC (25, 26), T_{FR} coexpress Blimp-1, which is known to repress CXCR5 expression (25, 30). Ablation of NFAT-2 in mice results in reduced expression of CXCR5 on T_{FR}, but not on T_{FH}, suggesting that this transcriptional factor may enable the proper localization of T_{FR} within B cell follicles, possibly by inhibiting Blimp-1–mediated repression of CXCR5 expression (31). T_{FR} restrict T_{FH} numbers and help to maintain a steady ratio of IgM^+ to IgM^- (switched) B cells (32) via IL-10 production (29); in vivo depletion of $CD4^+$ T cells with suppressive activity including T_{FR}, or in vivo blockade of IL-10 or TGF-β receptors results in T_{FH} expansion, loss of normal proportion of IgM^- B cells, and in increased levels of high-affinity Abs (26, 29, 33). A hallmark of HIV and SIV infection is the immune dysfunction of humoral responses characterized by loss of memory B cells and hypergammaglobulinemia (34, 35). T_{FH} frequency is significantly increased in the lymph nodes of HIV-infected individuals and chronically SIV_{mac251}-infected macaques (8, 36). Production of the IL-21 cytokine by T_{FH} is significantly reduced during HIV/SIV infection, possibly affecting GC homeostasis and the development of effective humoral responses to the virus (37). The HIV/SIV-associated changes in T_{FH} number and function may contribute to the impairment of B cell responses (9, 36, 38); however, other studies have found associations between the levels

*Animal Models and Retroviral Vaccine Section, National Cancer Institute, National Institutes of Health, Bethesda, MD 20892; †California National Primate Research Center, University of California Davis, Davis, CA 95616; ‡Department of Microbial Pathogenesis, University of Maryland School of Dentistry, Baltimore, MD 21201; and §Biostatistics and Data Management Section, National Cancer Institute, National Institutes of Health, Bethesda, MD 20852

[1]Current address: Department of Molecular and Translational Medicine, University of Brescia, Brescia, Italy.

Received for publication October 23, 2014. Accepted for publication July 13, 2015.

This work was supported entirely by the Intramural Research Program at the National Cancer Institute, National Institutes of Health.

Address correspondence and reprint requests to Dr. Monica Vaccari, National Cancer Institute, Animal Models and Retroviral Vaccine Section, 9000 Rockville Pike, Building 41, Room C303, National Institutes of Health, Bethesda, MD 20892. E-mail address: vaccarim@mail.nih.gov

The online version of this article contains supplemental material.

Abbreviations used in this article: DP, double-positive; GC, germinal center; lin, lineage; PD-1, programmed death 1; T_{FH}, T follicular helper cell; T_{FR}, T follicular regulatory cell; T_{REG}, T regulatory cell.

of functional T_{FH} and broadly neutralizing Abs in chronic HIV patients (39). Although the relative role of T_{FH} in HIV pathogenesis needs further investigation, it would be important to understand the molecular and cellular mechanisms that regulate T_{FH} expansion.

T_{FR} dynamics in HIV infection has not been investigated yet. We identified T_{FR} as $CXCR5^+$ T_{REG} in the lymph nodes of rhesus macaques, a well-established model of HIV infection. We show that 1) T_{FR} are infected by SIV_{mac251}, 2) there is an apparent decrease in T_{FR} levels, particularly during chronic infection, 3) T_{FR} levels are associated with the levels of T_{FH} and the total frequency of IgG^+ B cells, and 4) T_{FR} levels are inversely correlated with the avidity of Abs to SIV gp120 protein. Taken together, these findings suggest a potential role for T_{FR} in modulating humoral responses against HIV/SIV.

Materials and Methods

Animals and challenge

All of the animals used in this study were colony-bred rhesus macaques (*Macaca mulatta*) obtained from Covance Research Products (Alice, TX). The animals were housed and maintained in accordance with the standards of the Association for the Assessment and Accreditation of Laboratory Animal Care. This study was carried out in strict accordance with the recommendations in the *Guide for the Care and Use of Laboratory Animals* of the National Institutes of Health. All surgery was performed under general anesthesia, and all efforts were made to minimize suffering. All macaques were negative for simian retrovirus, simian T cell leukemia virus type 1, and herpesvirus B. Macaques were infected with a single high dose (6300 50% tissue culture-infective dose) (40) or with 10 repeated low doses (120 50% tissue culture-infective dose) of SIV_{mac251} given rectally (41) (see Table I).

Cell isolation from lymph nodes and mucosa

Cells were isolated from blood, lymph nodes, and spleen by density gradient centrifugation. Tissues from the rectum, jejunum, and colon were treated with 1 mM ultrapure DTT (Invitrogen Life Technologies) for 30 min followed by incubation in calcium/magnesium-free HBSS (Invitrogen Life Technologies) for 60 min with stirring at room temperature to remove the epithelial layer. Lamina propria lymphocytes were separated by cutting the tissue into small pieces and incubating in 10% FBS IMDM (Invitrogen Life Technologies) with collagenase D (400 U/ml; Boehringer Mannheim) and DNase (1 μg/ml; Invitrogen Life Technologies) for 2.5 h at 37°C. Mononuclear cells were placed over 42% Percoll (GE Healthcare) and centrifuged at 800 × *g* for 25 min at 4°C. Lamina propria lymphocytes were collected from the cell pellet (42).

Abs and staining

We used the following Abs: CD3–Alexa Fluor 700 (SP34-2), CD4-PerCP-Cy5.5 (L200), CD95-PE-Cy5 (DX2), CD197-PE-Cy7 (CCR7, clone 3D12), CD25-allophycocyanin-Cy7 (M-A251), CD195-PE (CCR5, clone 3A9), CD14–Alexa Fluor 700 (M5E2), CD16–Alexa Fluor 700 (3G8), CD56–Alexa Fluor 700 (B159), IgM-PerCP-Cy5.5 (G20-127), IgG-Qdot605 (G18-145), Ki67-PE (B56), and CD21-PE-Cy7 (B-ly4), all from BD Biosciences; Bcl-6-PE (IG191E/A8), CD278–Pacific Blue (ICOS, clone C398.4A), CD25–Pacific Blue (BC96), PD-1–allophycocyanin (EH12.2H7), CD39-BV421 (MOCP-21), and CD39 (A1) from BioLegend; Foxp3-FITC (PCH101), CXCR5-PE–eFluor 610 (MU5UBEE), and CD20-Qdot650 (2H7), all from eBioscience; and CD103-FITC (α_E integrin, clone 2G5), CD19-PE-Cy5 (J3-119), and CD127-PE (eBioRDR5) from Beckman Coulter. The $\alpha_4\beta_7$ Ab (Act-1) was obtained through the National Institutes of Health Nonhuman Primate Reagent Resource Program (AIDS Reagent Program, Division of AIDS, National Institute of Allergy and Infectious Diseases, National Institutes of Health). Vivid amine-reactive dye was used to discriminate live/dead cells (Invitrogen). IgA-Texas Red (polyclonal) was obtained from SouthernBiotech, and CD38-FITC (clone AT-1) was from StemCell Technologies.

For phenotypic characterization of $CD4^+$ T cells subsets, cells were stained with surface markers CD3, CD4, CD95, CD25, CCR7, CXCR5, ICOS and Vivid. Cells were then fixed and permeabilized according to eBioscience's instructions and stained with anti-Foxp3 and anti–Bcl-6 for 30 min. The appropriate isotype-matched control Ab was used to define positivity. T_{FR} cells were gated as live $CD3^+CD4^+CD95^+$ T cells, and their percentage was calculated as the frequency of $CXCR5^+$ and $CCR7^-$ within $Foxp3^+CD25^+$ cells (percentage of T_{REG}) or within $CD95^+CD4^+$ T cells (percentage of memory $CD4^+$ T cells) (26). Similarly, double-positive (DP) cells were $CXCR5^+$ and $CCR7^+$ cells and $CCR7^+$ T_{REG} were $CXCR5^-$ and $CCR7^+$. Finally, T_{FH} were gated as $CXCR5^+PD\text{-}1^{hi}$ cells within the $Foxp3^-$ region or the memory $CD4^+$ T cells population (see Fig. 1A).

B cells were gated as live/lineage $(lin)^-$ $(CD3^-CD14^-CD16^-CD56^-)$ positive for CD20 and or CD19 markers. For plasmablasts, cells were stained with lineage markers CD20, CD38, CD39, IgM, IgG, and IgA. Cells were treated with Cytofix/Cytoperm (BD Biosciences) and stained with Ki67. Plasmablasts were gated as lin^- $(lin^-CD20^+$ and/or $CD19^+CD21^-$ $Ki67^+CD38^+CD39^+)$ (43).

Marker expression was analyzed with an LSR II flow cytometer using FACSDiva software (BD Biosciences). FACS analysis was performed using FlowJo software (Tree Star, Ashland, OR). A minimum of 10,000 cells per tube were analyzed.

$CD4^+$ T cells counts

The absolute number of $CD4^+$ T cells was calculated as previously described (44).

Sorting

To determine the RNA levels for IL-10, TGF-β, and SIV DNA, cells from lymph nodes were stained with Vivid, CD3, CD4, CD25, CCR7, and CXCR5. T_{FR} were defined as live $CD3^+CD4^+CD25^+CXCR5^+CCR7^-$; T_{REG} were defined as $CXCR5^-CCR7^+$.

For proliferation, $CD25^+CD4^+$ T cells (live $CD3^+CD4^+CD25^+$) were sorted. Sorting was performed on a FACSAria (BD Biosciences).

Migration assay

Sorted live $CD3^+CD4^+CD25^+$ cells were migrated for 1 h to 1 μg/ml CXCL13 (R&D Systems, catalog no. 801-CX/CF) using 5-μm-pore polycarbonate membrane inserts (Millipore).

Proliferation

Cell proliferation was determined by dilution of CFSE (Life Technologies). Briefly, CD25-depleted $(CD3^+CD4^+)$ cells were stained with CFSE for 10 min and were then placed in a 24-well plate in the presence or absence of CD3 (10 μg/ml; clone FN18) with soluble anti-CD28 (1 μg/ml; clone CD28.2), in the presence or absence of autologous $CD3^+CD4^+CD25^+$ cells migrated to CXCL13 (10:1 ratio), for 4 d. Cells were then stained and analyzed by FACS as described above.

Cyclosporin A in vitro treatment

Cells from lymph nodes were incubated 30 h with 50 μg cyclosporin A (Sigma-Aldrich) and incubated for 6 h with or without PMA and in the presence of brefeldin A (GolgiPlug; BD Biosciences).

RT-PCR

Total RNA was extracted from whole tissue with RNeasy Plus (Qiagen) and reverse transcribed with a high-capacity cDNA reverse transcription kit (Applied Byosystems). After reverse transcription, the relative amounts of transcripts were determined by real-time PCR with the SYBR Green quantitative PCR master mix (Promega) using 0.2 μM PCR primers for IL-10 (forward, 5′-AGAACCACGACCCAGACATC-3′, reverse, 5′-GGCCTTGC-TCTTGTTTTCAC-3′) and TGF-β. The TGF-β was described elsewhere (45). Quantification of cDNA was normalized in each reaction according to the internal β-actin control (forward, 5′-GGCACCCAGCACAATGAAG-3′, reverse, 5′-GCTGATCCACATCTGCTGG-3′). A real-time nucleic acid sequence–based amplification assay was used to quantitative SIV RNA in plasma (46). SIV DNA was quantified as previously described (40).

Immunohistochemistry in lymph nodes

The primary Abs included anti-Foxp3 (Abcam, rabbit), anti-CD20 (Dako, Carpinteria, CA; mouse Ig2a), and anti-CD3 (UCD, rat). TBS with 0.05% Tween 20 was used for all washes. Ab diluent (Dako) was used for all Ab dilutions. For all primary Abs, slides were subjected to an Ag retrieval step consisting of incubation in AR10 (BioGenex, San Ramon, CA) for 2 min at 125°C in a digital decloaking chamber (Biocare Medical, Concord, CA) followed by cooling to 90°C before rinsing in water. Primary Abs were replaced by normal rabbit IgG, mouse IgG (Invitrogen, Grand Island, NY), and rat IgG (Vector Laboratories, Burlingame, CA) and were included with each staining series as the negative control. Nonspecific binding sites were blocked with 10% goat serum and 5% BSA (Jackson ImmunoResearch Laboratories, West Grove, PA). Binding of the primary Abs was detected

simultaneously using Alexa Fluor 568 goat anti-rat, Alex Fluor 647 goat anti-mouse IgG2a, and Alex Fluor 488 goat anti-rabbit. All slides were coverslipped using ProLong Gold with DAPI (Molecular Probes, Grand Island, NY) to stain nuclei. All the control experiments gave appropriate results with minimal nonspecific staining.

Slides were visualized with epifluorescent illumination using a Zeiss Axioplan 2 microscope (Carl Zeiss, Thornwood, NY) and appropriate filters. Digital images were captured and analyzed by using Openlab software (Inprovision, Waltham, MA). Alexa Fluor 647 was captured in a black-and-white channel whereas other fluorescence dyes were pictured in color channels. Five high-power (×40) microscope fields were randomly chosen and captured digitally with the system described above. Each captured field includes an area of ~0.04 mm^2. Only clearly positive cells with distinctly labeled nuclei (DAPI) and bright staining were considered positive. Individual positive cells in the five captured high-power microscope fields of the immunohistochemical stained tissue sections were counted manually by a single observer. The numbers of positive cells are presented as cells per square millimeter.

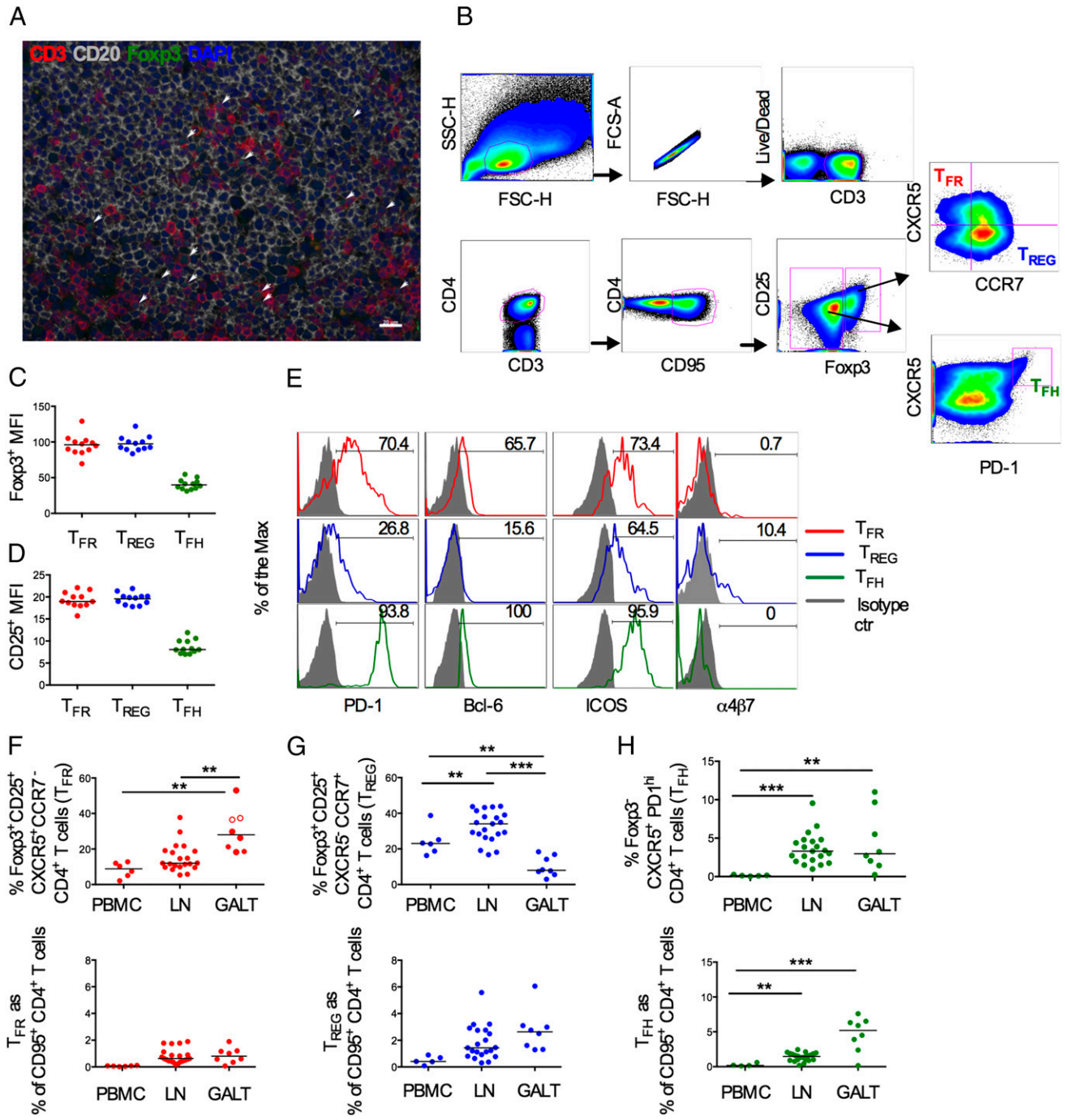

FIGURE 1. Characterization and distribution of T_{FR} in SIV-uninfected macaques. (**A**) DP $CD3^+$ (red) and $Foxp3^+$ cells (green) are present in B follicles (CD20 in gray) in lymph nodes from a naive macaque (blue, DAPI; scale bar, 20 μm). (**B**) Representative flow cytometry plots showing the gating strategy for T_{FR}, $CCR7^+$ T_{REG}, and T_{FH} in lymph nodes. All the subsets were gated on singlet/live/$CD3^+CD4^+CD95^+$. T_{FR} and $CCR7^+$ T_{REG} were identified as $Foxp3^+$ $CD25^+$ and $CXCR5^+CCR7^-$ or $CXCR5^-CCR7^+$, respectively; T_{FH} were identified as $Foxp3^-CXCR5^+PD\text{-}1^{hi}$. (**C**) Geometric mean (mean fluorescence intensity [MFI]) of Foxp3 and (**D**) CD25 expression. (**E**) Cell surface expression of PD-1, Bcl-6, ICOS, and $\alpha_4\beta_7$ in T_{FR} (red), T_{REG} (blue), and T_{FH} (green). Isotype controls are in gray. Frequency of (**F**) $CXCR5^+$ and $CCR7^-$ cells and (**G**) $CXCR5^-$ and $CCR7^+$ cells within $Foxp3^+CD25^+CD4^+$ T (*upper panel*) or within memory $CD4^+$ T cells (corresponding *lower panels*) in blood, peripheral lymph nodes, and in the GALT (colon, jejunum, and rectal mucosa) of naive animals. The median is shown. (**H**) T_{FH} frequency on $Foxp3^-$ (*upper panel*) and memory $CD4^+$ T cells (*lower panel*) in different tissues.

Avidity assay

Avidity was analyzed as previously described (41). Briefly, recombinant SIV gp120 protein made from codon-optimized SIV$_{mac239}$ gp120 fused to the C-terminal tag of HIV-1 gp120 was used as an Ag for the capture ELISA to detect SIV Abs against conformational epitope. Ab avidity was determined by parallel ELISA. Heat-inactivated plasma samples were serially diluted and applied to a 96-well plate capturing SIV$_{mac239}$ gp120. After 1 h of incubation, the plate was washed and half the samples were treated with TBS, whereas the paired samples were treated with 1.5 M sodium thiocyanate (Sigma-Aldrich) for 10 min at room temperature. The plate was washed and a goat anti-monkey IgG-detecting Ab (Fitzgerald) was used. The avidity index (%) was calculated by taking the ratio of the sodium thiocyanate–treated plasma dilution giving an OD of 0.5 to the TBS-treated plasma dilution giving an OD of 0.5 and multiplying by 100. Plasma of uninfected normal macaques served as negative controls.

Statistical analysis

Tests of two groups of animals for differences between cell types, tissues, or stages of infection were performed using the exact Wilcoxon rank sum test. Differences before and after infection within the same group of animals were assessed using the Wilcoxon signed rank test. Differences across three stages of infection were modeled using repeated measures ANOVA when distributional assumptions were met. Correlation analyses were performed using the exact Spearman rank correlation method. Trends across three groups were assessed by the Jonckheere–Terpstra test. Owing to the exploratory nature of this study, the p values reported were not corrected for multiple comparisons. The p values ≤ 0.05 were considered statistically significant, and we note that for outcomes where all pairwise comparisons of three groups are possible, the p values ≤ 0.02 remain significant after correction for the multiple tests.

Results

Characterization and tissue distribution of T_{FR} in naive rhesus macaques

T_{FR} localize in the GC of mice and humans (25, 26, 29, 47). We confirmed the presence of Foxp3$^+$CD3$^+$ T cells in healthy macaque's B cell follicles of lymph nodes by immunohistochemistry (Fig. 1A). We then characterized T_{FR} in cell suspension by flow cytometry and compared their frequency, phenotype, and localization to those of CCR7$^+$ T_{REG} and T_{FH}. The gating strategy used to define these three cell subsets is shown in Fig. 1B. T_{FR} and T_{REG} were gated within the live Foxp3$^+$CD25$^+$CD95$^+$CD4$^+$ T cells and defined as CXCR5$^+$ and CCR7$^-$, consistent with GC location, and as CXCR5$^-$ and CCR7$^+$, consistent with T zone location (Fig. 1B). Of note, the T_{REG} population identified by this strategy only includes a specific subset based on the expression or the lack thereof of the two considered chemokines. We refer to this subset as CCR7$^+$ T_{REG} or T_{REG} for simplicity.

In agreement with Sage et al. (48) and Linterman et al. (25), we used the Foxp3 marker to distinguish between T_{FH} and T_{FR} subsets because both populations express CXCR5, PD-1, ICOS, and Bcl-6. T_{FH} were defined as Foxp3$^-$CXCR5$^+$PD-1^{hi}CD4$^+$ T cells (Fig. 1B).

Consistent with their mouse counterpart, macaque T_{FR} expressed comparable levels of Foxp3 (Fig. 1C), equal intensity and frequency of CD25, and frequency of CD39 to T_{REG} (Fig. 1D, Supplemental Fig. 1A, 1B) (25, 26). T_{FR} were also negative for CD127, the marker for the IL-7 receptor, and expressed common T_{FH} markers, such as PD-1, Bcl-6, and ICOS (Fig. 1E, Supplemental Fig. 1C) (28). Only a subset of T_{REG} but not of T_{FR} or T_{FH} was positive for the α_E (CD103) and $\alpha_4\beta_7$ integrin (25, 26) (Fig. 1E and data not shown).

Within the Foxp3$^+$CD25$^+$ population we identified an additional CXCR5$^+$CCR7$^+$ DP cell subset (Fig. 1B). DP cells expressed intermediate levels of PD-1 as compared with T_{FR} and T_{REG} and had equal levels of Bcl-6 to T_{FR} (Supplemental Fig. 1D).

We looked at the distribution of T_{FR}, T_{REG}, and T_{FH} in blood, peripheral lymph nodes, and in the GALT (colon, jejunum, and rectal mucosa) obtained from 6, 21, and 8 naive macaques, respectively (Fig. 1F–H). Representative flow plots obtained from blood, lymph node, and rectal mucosa tissue from one healthy animal are shown in Supplemental Fig. 1E. T_{FR} were mainly in the GALT and

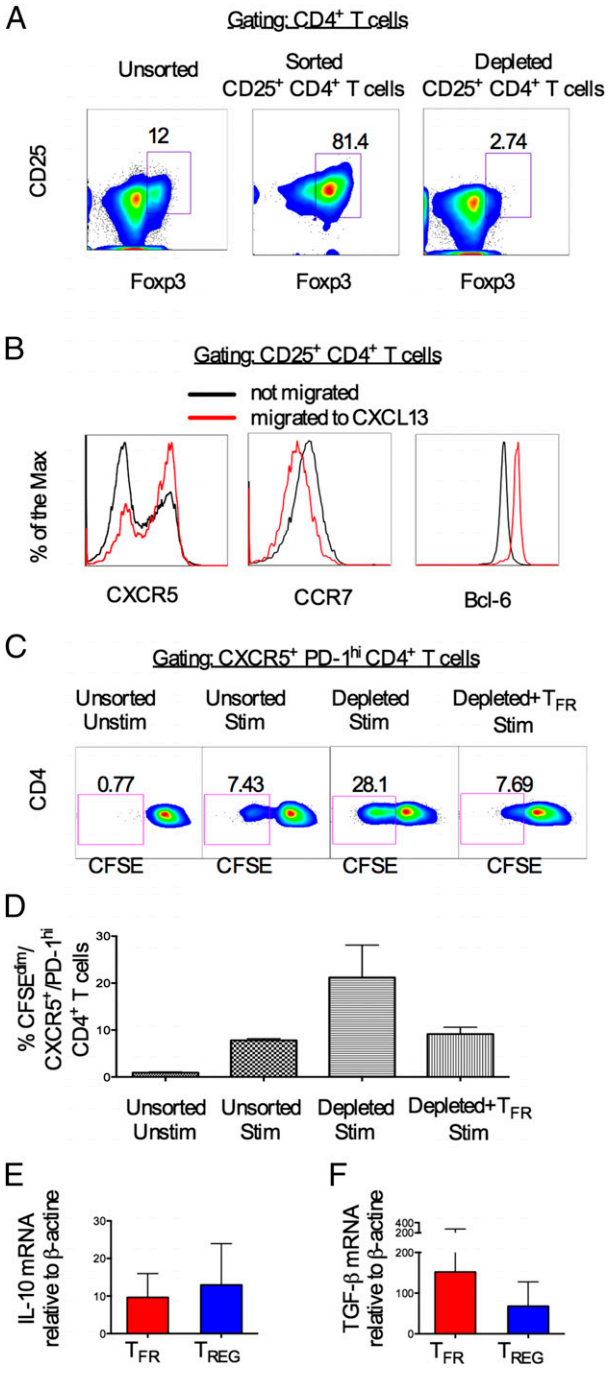

FIGURE 2. T_{FR} suppress in vitro T_{FH} cell proliferation. (**A**) Representative density plot showing unsorted (*upper panel*), sorted CD25$^+$CD4$^+$ T cells (*middle panel*), and CD25$^+$CD4$^+$ T-depleted cells (*lower panel*) from a lymph node of a naive macaque. (**B**) Cell surface expression of CXCR5, CCR7, and Bcl-6 on CD4$^+$ T cells that migrated (red line) or did not migrate (black line) to CXCL13. (**C**) Representative density plot showing proliferation (CFSE^{dim}) of stimulated (CD3, CD28) unsorted, CD25$^+$ depleted CD4$^+$ T cells alone or cocultured with CXCL13 migrated CD25$^+$CD4$^+$ T cells. (**D**) Percentage of proliferating CXCR5$^+$PD-1^{hi}CD4$^+$ T cells in all conditions. The bars represent the mean ± SE. (**E**) *IL-10* and (**F**) *TGF-β* mRNA measured by RT-PCR from T_{FR} and CCR7$^+$ T_{REG} sorted from lymph nodes of four naive animals. The bars represent the mean ± SE.

lymph nodes and only a few were detected in blood (Fig. 1F, Supplemental Fig. 1E). Within the Foxp3$^+$CD25$^+$ population, cells that expressed only CXCR5 were less frequent in lymph nodes than in the GALT ($p < 0.0001$ by the Wilcoxon rank sum test; Fig. 1F, *upper panel*), and the opposite was observed for cells that expressed only CCR7 ($p < 0.0001$ by the Wilcoxon rank sum test; Fig. 1G, *upper panel*). The apparent difference in tissue distribution in lymph nodes and GALT was lost when we looked at the frequency of T_{FR} and T_{REG} within the memory CD4$^+$ T cell population (*lower panels* in Fig. 1F, 1G). DP cells were equally distributed among all the tissues analyzed, including the blood (Supplemental Fig. 1F). Finally, T_{FH} frequency was significantly higher in lymph nodes and in the GALT than in the blood, as previously described (PBMC versus lymph node, $p < 0.0001$; PBMC versus GALT, $p = 0.0031$) (49) (Fig. 1H).

Because we could not determine whether DP cells home exclusively to the B zone, we excluded them from the rest of the analysis.

Macaque T_{FR} suppress CD4$^+$ T cells and T_{FH} proliferation of in vitro

In mice, T_{FR} control T_{FH} numbers and decrease their proliferation in vivo and in vitro (26). We studied whether macaque lymph nodes also contained a suppressive CD4$^+$ T cell population that homes to the B follicles. We sorted CD4$^+$CD25$^+$ live cells from the lymph nodes of two naive animals and isolated those capable of migrating in response to CXCL13, the ligand for CXCR5 (Fig. 2). Although we could not use Foxp3, an intracellular marker, to discriminate suppressor CD4$^+$ T cells, sorted CD25$^+$CD4$^+$ T cells from lymph nodes consisted primarily of Foxp3$^+$CD4$^+$ T cells (Fig. 2A). Regulatory CD4$^+$ T cells that migrated to CXCL13 had higher levels of CXCR5, lower levels of CCR7, and expressed higher levels of Bcl-6 than did those that did not migrate (Fig. 2B). This strategy allowed us to obtain a population of CD4$^+$ T cells, highly enriched for T_{FR}, which could be used in downstream functional assays. Unsorted and sorted cells were stimulated with or without CD3 and CD28, in the presence or absence of migrated CD25$^+$ CD4$^+$ T cells (follicular T_{REG}–

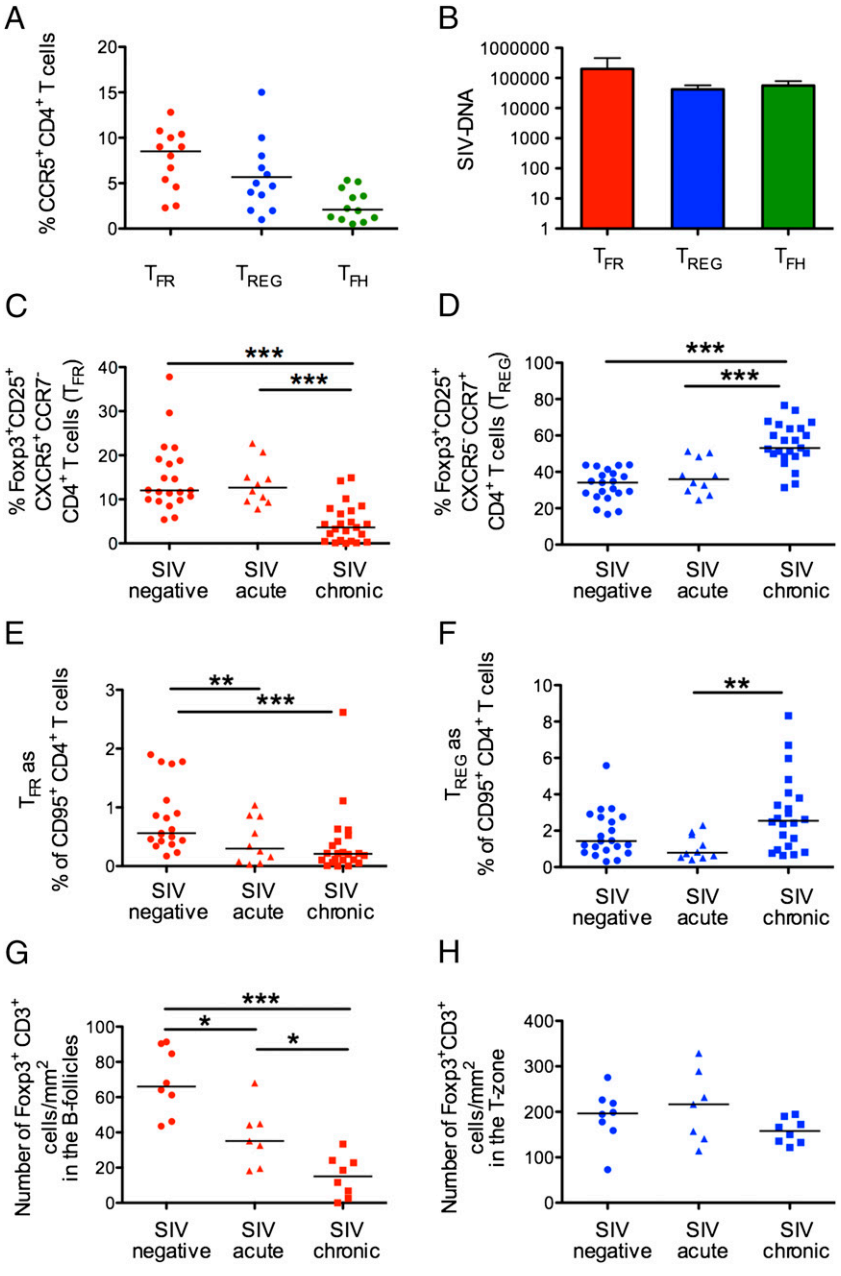

FIGURE 3. T_{FR} susceptibility and dynamics during SIV chronic infection. (**A**) Percentage of CCR5$^+$ T_{FR}, CCR7$^+$ T_{REG}, and T_{FH}. (**B**) SIV DNA levels in sorted T_{FR}, CCR7$^+$ T_{REG}, and T_{FH} by PCR. (**C**) Frequency of T_{FR} and (**D**) CCR7$^+$ T_{REG} within Foxp3$^+$ CD25$^+$ cells, and (**E**) T_{FR} and (**F**) CCR7$^+$ T_{REG} within memory CD4$^+$ T cells in lymph nodes of naive and acutely and chronically SIV-infected macaques. (**G**) Number of Foxp3$^+$CD3$^+$ cells in the B follicles (T_{FR}) and (**H**) in the T zone (T_{REG}) of intact lymph nodes from naïve and acutely and chronically infected macaques.

enriched population). We assessed proliferation (percentage of $CFSE^{dim}$ cells) within $CXCR5^+PD\text{-}1^{hi}CD4^+$ T cells (T_{FH}-gated cells) by FACS analysis. Representative plots of the gated $CXCR5^+$ $CD4^+$ T cells (gate 1) are shown in Supplemental Fig. 2A. Interestingly, T_{FH} proliferated less in the presence of T_{FR}-enriched cells following stimulation than in the absence of $CD25^+$ cells, as shown in the representative plots in Fig. 2C and graphically in Fig. 2D. As expected, T_{FR} also reduced non-T_{FH} $CD4^+$ T cell subset proliferation (gate 2) (Supplemental Fig. 2B).

Consistent with their regulatory function and similar to T_{REG}, T_{FR} produce IL-10 and TGF-β, which together suppress the proliferative potential and function of $CD4^+$ T cells in mice (50, 51). Thus, we measured the levels of IL-10 and TGF-β in enriched populations of T_{FR} ($CD3^+CD4^+CD25^+CXCR5^+CCR7^-$) and $CCR7^+$ T_{REG} ($CD3^+CD4^+CD25^+CXCR5^-CCR7^+$) obtained from peripheral lymph nodes of three naive macaques. T_{FR} had equivalent IL-10 and TGF-β mRNA levels, by RT-PCR, than $CCR7^+$ T_{REG} (Fig. 2E, 2F).

SIV_{mac251} infection and T_{FR} frequency

Sorted T_{FR} and T_{REG} from lymph nodes of four chronically infected macaques expressed comparable levels of CCR5 (Fig. 3A) and harbored equivalent levels of SIV DNA (Fig. 3B). Similar SIV DNA levels were also found in T_{FH} cells.

We analyzed the effect of SIV_{mac251} infection on the frequency of T_{FR} and $CCR7^+$ T_{REG} in the lymph nodes of 10 acutely (2 or 3 wk postinfection) and 23 chronically infected (12–15 wk postinfection) macaques (Fig. 3C, 3D, Table I). Representative dot plots for two macaques before and after infection are shown in Supplemental Fig. 3A. Cells expressing only $CXCR5^+$ were significantly reduced within the $Foxp3^+CD25^+$ population during chronic infection (chronic versus negative, $p < 0.0001$; chronic versus acute, $p < 0.0001$) (Fig. 3C), whereas CCR7 single-positive cells simultaneously increased (chronic versus negative, $p < 0.0001$; chronic versus acute, $p = 0.0003$) when compared with noninfected and chronically infected animals (Fig. 3D).

We looked at the levels of T_{FR} and $CCR7^+$ T_{REG} with respect to the memory $CD95^+CD4^+$ T population. T_{FR} showed a downward trend from negative to acute to chronic ($p = 0.0005$ by the Jonckheere–Terpstra test for trend), with marginal differences in acute (negative versus acute, $p = 0.049$) and a significant decrease in chronic infection (negative versus chronic, $p = 0.0003$) (Fig. 3E). $CCR7^+$ T_{REG} levels showed an increasing trend after infection and significance was reached between the values detected in acute and in chronic phase ($p = 0.0018$) (Fig. 3F).

We performed immunohistochemistry in lymph nodes at 3 and 12 wk postinfection from seven and eight animals, respectively (Fig. 3G, 3H). The numbers of $CD3^+$ cells expressing Foxp3 in the B cell follicles was significantly reduced in acute infection ($p = 0.0022$, $n = 7$) and contracted even further in chronic infection ($p < 0.0001$, $n = 8$), when compared with naive ($n = 8$) animals (Fig. 3G, Supplemental Fig. 3B). The number of $Foxp3^+CD3^+$ cells in the T zone did not change, as described by others (Fig. 3H) (52).

We did not see any significant correlation between the frequency of T_{FR} or T_{REG} and the SIV RNA plasma levels (data not shown).

To further explore possible mechanisms for the SIV-associated decrease of T_{FR}, we looked at markers of immune activation. We could not find any association with the frequency of $Ki67^+CD4^+$ T cells in lymph nodes of 10 chronic animals (data not shown).

Table I. Serological data for acute and chronically infected animals

	Challenge	Weeks p.i.	VL	CD4 Count
Acute				
P061	High dose i.r.	2	5,806,601	748
P066	High dose i.r.	2	25,556,960	489
P074	High dose i.r.	2	30,925,780	333
P136	High dose i.r.	2	39,844,500	382
P273	High dose i.r.	2	34,856,014	524
P251	Low dose i.r.	3	115,008,398	647
P434	Low dose i.r.	3	215,693,077	517
P650	Low dose i.r.	3	23,469,446	489
P716	Low dose i.r.	3	108,209,623	454
P712	Low dose i.r.	3	49,568,224	757
Chronic				
P015	High dose i.r.	14	121,368	485
P061	High dose i.r.	14	368,663	928
P074	High dose i.r.	14	11,883,300	437
P134	High dose i.r.	14	16,963,740	260
P136	High dose i.r.	14	19,165,270	340
P266	High dose i.r.	15	172,649	265
P273	High dose i.r.	15	163,587	360
P274	High dose i.r.	15	1,297,398	265
E060	Low dose i.r.	14	4,957,329	Nd
E074	Low dose i.r.	14	Nd	Nd
P632	Low dose i.r.	12	7,825,190	111
P761	Low dose i.r.	15	31,347	1330
P758	Low dose i.r.	15	24,934	1431
P760	Low dose i.r.	15	1,425,169	426
R158	Low dose i.r.	15	1,440,103	820
P733	Low dose i.r.	15	1,358,565	212
P746	Low dose i.r.	15	143,386	618
P754	Low dose i.r.	15	2,168,071	734
P698	Low dose i.r.	15	21,182,252	572
P609	Low dose i.r.	15	5,462,462	239
P251	Low dose i.r.	15	111,656	406
P633	Low dose i.r.	15	1,104,050	514
P761	Low dose i.r.	15	147,114	1330

For viral load (VL), SIV/RNA copies/ml plasma are shown. For $CD4^+$ count, absolute $CD4^+$ T cell numbers/mm^2 blood are shown. i.r., intrarectally; p.i., postinfection.

In mice NFAT-2 is critical for the upregulation of CXCR5 on T_{FR} (31), hence for their migration to the GC. Thus, NFAT-2 may be involved in the reduction of T_{FR} during chronic infection. To determine whether CXCR5 expression on macaque T_{FR} was also dependent on NFAT activity, we treated lymph nodes cells from two naive animals with cyclosporin A and measured changes in the CXCR5 and CCR7 levels within $Foxp3^+CD25^+CD4^+$ T cells (Supplemental Fig. 3C, 3D). Although cyclosporin A treatment had no effect on CCR7, it decreased CXCR5 expression levels on $Foxp3^+CD25^+CD4^+$ T cells.

Decreased T_{FR} and increased T_{FH} frequency during SIV_{mac251} infection

The decrease of $CXCR5^+$ regulatory T cells may be associated with T_{FH} expansion during SIV_{mac251} infection. We measured the frequency of T_{FH} in lymph nodes of infected macaques as shown in Fig. 1B. The percentage of T_{FH} cells within the memory $CD4^+$ T cell population did not change during acute infection, but this population significantly expanded during chronic infection (weeks 12–15 after infection), as described by others (8) (negative versus chronic and acute versus chronic, $p < 0.0001$) (Fig. 4A, 4B). Of note, we found a significant inverse correlation between the levels of T_{FR} and T_{FH} on memory $CD4^+$ T cells during acute and chronic infection ($R = -0.82$, $p = 0.0058$ and $R = -0.69$, $p = 0.0010$ by the Spearman rank test) (Fig. 4B, 4C).

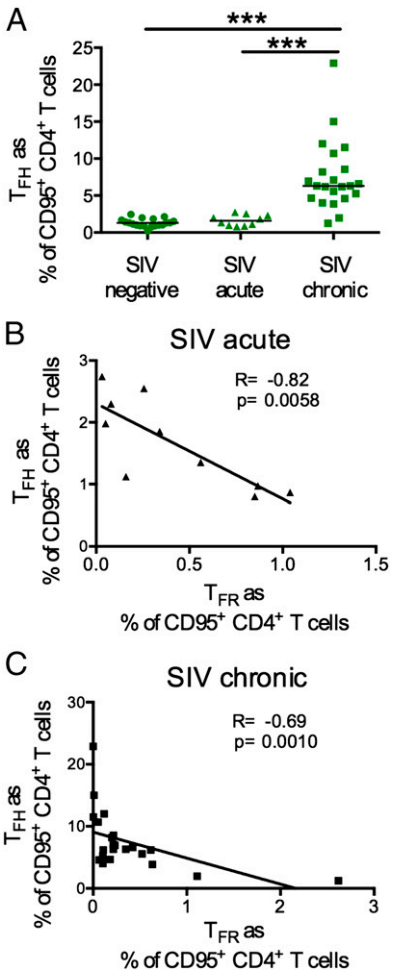

FIGURE 4. Association between T_{FR} and T_{FH} levels in SIV infection. (**A**) Frequency of T_{FH} on memory $CD4^+$ T cells in lymph nodes of naive and acutely and chronic SIV-infected macaques. (**B**) Correlation between the percentage of T_{FR} and T_{FH} on memory $CD4^+$ T cells in acute and (**C**) chronic infection.

T_{FR} frequency correlates with decreased avidity of Abs to the gp120

In mice, T_{FR} cells play a role in reducing plasma cell differentiation (26). We measured the frequency of IgM^+, IgG^+, or IgA^+ $CD20^+$ B cells and plasmablasts, defined as lin^- ($CD3^-CD14^-CD16^-CD56^-$) $CD20^+$ and/or $CD19^+$ and $CD21^-Ki67^+CD38^+CD39^+$ in lymph nodes of SIV_{mac251} chronically infected animals ($n = 14$) by flow cytometry. Whereas we did not find any associations with the frequency of total memory B cells or plasmablasts measured in lymph nodes, we found a weak negative correlation between the frequency of IgG^+ B cells and the frequency of IgM-switched plasmablasts (IgG^+ and IgA^+) with the percentage of T_{FR} within $Foxp3^+CD25^+$ cells (Fig. 5A, 5B).

T_{FH} are associated with the avidity to influenza virus and SIV (8, 53). In SIV_{mac251}-infected macaques, avidity to the gp120 is low during acute infection and increases during chronic infection (Fig. 5C). We confirmed that T_{FH} were positively associated with gp120 avidity when all the infected macaques were considered ($R = 0.88$, $p = 0.0031$; Fig. 5D), but not when the acute and chronic phases values were looked at separately. Importantly, T_{FR} levels on memory $CD4^+$ T cells were associated with a reduction of binding high avidity Abs to SIV gp120 in all the infected animals ($R = -0.85$, $p = 0.0061$) and in chronic phase ($R = -1.0$, $p = 0.017$), but not during the acute phase ($R = -0.80$, $p = 0.33$) (Fig. 5E, 5F and data not shown).

Discussion

In this study we identified T_{FR} in lymphoid tissues of healthy nonvaccinated rhesus macaques. We confirmed the presence of $Foxp3^+$ T cells in the B zone of intact lymph nodes of macaques. Because T_{FR} share markers of T_{FH} and T_{REG}, they have been isolated and functionally characterized in mice as T_{FH} positive for Foxp3 (25) or, alternatively, as "follicular" T_{REG} expressing CXCR5 (26, 47). We opted for the latter identification strategy to characterize macaque T_{FR} in lymph nodes. Additionally, we identified a subset of CCR7-expressing T_{REG} that are $CXCR5^-$ and, therefore, in principle are unable to enter the GC, and another subset of $CXCR5^+$ and $CCR7^+$ T_{REG} (DP). Because it is possible that DP cells may localize at the T/B borders/mantle zone, following gradients of CXCL13 (B cell follicles, GC) and of CCL21 and CCL19 (T zone), we excluded this population from our analysis (7).

In accordance with their mouse counterpart, macaque T_{FR} expressed high levels of PD-1, ICOS, and Bcl-6, they were $CD39^+$ and $CD127^-$, and they mainly resided in the GALT and lymph nodes. In a few macaques, T_{FR} had similar levels of IL-10 and TGF-β mRNA as did $CCR7^+$ T_{REG} (25, 26). It is possible that IL-10 and TGF-β may play a role in the T_{FR}-mediated control of T_{FH} proliferation, as shown in mice. We did not directly assess the suppressive ability of sorted $CD25^+CXCR5^+CCR7^-$ cells; however, lymph nodes of healthy noninfected macaques contained a $CXCR5^{hi}CCR7^{lo}Bcl\text{-}6^{hi}CD25^+CD4^+$ population displaying in vitro chemotaxis toward CXCL13, as well as suppressive activity on $CD4^+$ T cells and T_{FH} proliferation. Further characterization is needed to confirm IL-10 and TGF-β production by macaque T_{FR} and their role in the apparent suppression of T_{FH} cells.

We took advantage of the established similarities between SIV infection of macaques and HIV-1 infection of humans to study T_{FR} susceptibility and dynamics during infection in comparison with $CCR7^+$ T_{REG}. Previous studies on $CD4^+$ T susceptibility have shown that $CD25^+Foxp3^+$ cells are less susceptible than other subsets to HIV/SIV infection owing to their anergic nature and to the

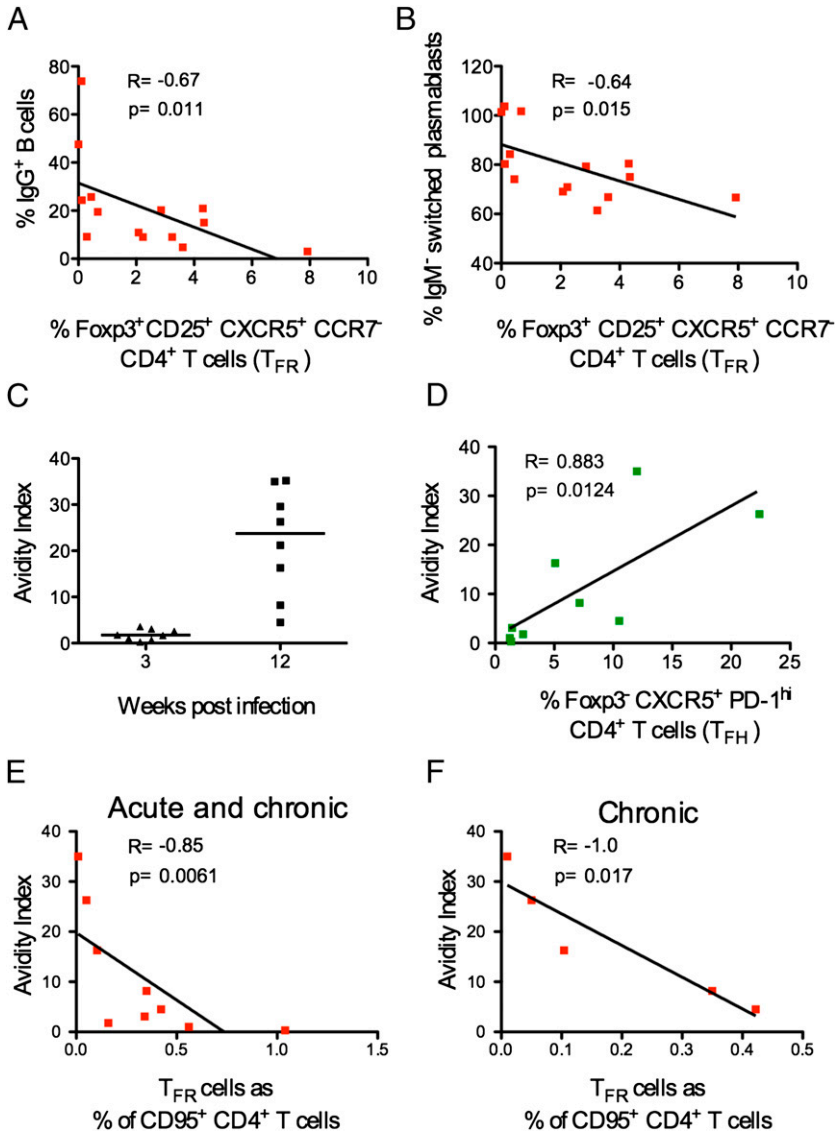

FIGURE 5. T_{FR} levels and SIV-specific Ab avidity. (**A**) Correlation between the frequency of T_{FR} on Foxp3$^+$CD25$^+$ cells and IgG$^+$ B cells or (**B**) switched IgM$^-$ plasmablasts in lymph nodes of chronically infected macaques. (**C**) Avidity index of plasma SIV gp120 IgG measured in acutely and chronically infected macaques (the median is shown). (**D**) Correlation between the frequency of T_{FH} or (**E**) T_{FR} and the avidity index in plasma of all the SIV-infected macaques and (**F**) in chronically infected macaques.

Foxp3-mediated inhibition of HIV-1 long terminal repeat activation (54–57). Therefore, the relative frequency of CD25$^+$Foxp3$^+$ CD4$^+$ T cells increases in acute and chronic HIV/SIV infection, whereas their absolute number remains the same (56, 58, 59). Similarly, we observed a trend for increased frequency of CCR7$^+$ T_{REG} within the memory CD4$^+$ population and no differences in the number of CD3$^+$Foxp3$^+$ cells in the T zone of intact lymph nodes in chronic infection.

T_{FR} from naive macaques expressed comparable levels of surface CCR5 to T_{REG} and had equivalent levels of SIV DNA following infection. Conversely, we saw a reduction in T_{FR} frequency and a decrease of CD3$^+$Foxp3$^+$ cells in the B follicles of infected animals, in particular during the chronic phase of infection. Whereas we could not discern between CD8$^+$ T cells and CD4$^+$ T cells in our immunohistochemical analysis, some chronically infected animals had negligible numbers of Foxp3$^+$ T cells in the GC, indicating an overall reduction of regulatory cells, likely including T_{FR}.

We could not determine whether T_{FR} are more susceptible to SIV$_{mac251}$ infection than T_{REG}, and we did not observe any association between the T_{FR} levels and viral replication levels or with immune activation.

The reduction in Foxp3$^+$ cells in the GC may be driven by SIV-associated changes in the homing patterns of these cells. NFAT-2 is an essential transcriptional factor for CXCR5 expression on mice T_{FR} (31). HIV envelope induces NFAT-2 translocation to the nucleus, where it binds to multiple sites within the HIV long terminal repeat (60, 61). HIV/SIV may therefore alter NFAT-dependent expression of CXCR5. We showed that cyclosporin A, a calcineurin inhibitor that blocks NFAT dephosphorylation, decreases CXCR5 levels on macaque CD4$^+$CD25$^+$Foxp3$^+$ cells, but we were unable to test this intriguing hypothesis in our model due to the lack of reagents that cross-react with macaque NFAT proteins.

T_{FH} numbers expand in acute and chronic viral infections, such as in influenza A virus infection in mice, and in chronic hepatitis B and HIV/SIV in humans and macaques (62–64). In particular during acute influenza A virus infection, a temporary T_{FH} expansion occurs 3 d after challenge (62). Differently, in HIV/SIV infection, a sustained expansion of T_{FH} is seen in chronic, but not during the acute phase, of infection, as we also observed in our study (8).

We found an association between the levels of T_{FR} and T_{FH} in acutely and chronic macaques infected with SIV$_{mac251}$. It is possible that a reduction or lack of expansion of T_{FR} may contribute to the increased T_{FH} number in chronic infection. Alternatively, the persistence of the Ag may lead to the increase in T_{FH}, resulting in higher levels of PD-1 in the GC and in T_{FR} reduction (47). Additionally, changes in T_{FR} function, other regulatory subsets in the GC (CD8$^+$

and NK T-cells), imbalanced cytokine milieu (i.e., increased IL-6), and immune activation are likely to participate in the HIV-associated increase in T_{FH} numbers (8, 19).

To our knowledge our study is the first to describe T_{FR} dynamics and changes in the T_{FH}/T_{FR} ratio during SIV infection, together with the study by Chowdhury et al. (65) reporting similar findings in SIV_{smE660}-infected macaques.

By suppressing T_{FH} numbers and proliferation, T_{FR} modulate B cell responses in mice (26, 29, 47). No correlation was found with the frequency of plasmablasts or with the IgA^+ B cells. We found an association between the relative frequency of $CXCR5^+$ cells within the $CD25^+Foxp3^+$ population and the frequency of total IgG^+ B cells and of overall switched IgM^- (IgA^+IgG^+) B cells and plasmablasts in lymph nodes (32).

The accumulation of T_{FH} in chronic SIV infection is associated with increased titers of higher avidity SIV-specific Igs (8). Interestingly, we observed an antithetic role of T_{FR} and T_{FH} in the avidity of Abs to the SIV gp120 protein throughout the infection, and only T_{FR} levels were strongly correlated with the increased avidity during chronic infection. It has been proposed that T_{FH} accumulation, together with HIV-associated changes in cell function, may lead to a reduction in affinity maturation due to a lowered competition for B cell selection. However, so far, the role of T_{FH} cells in HIV/SIV pathogenesis has been studied without making a clear distinction between T_{FR} and T_{FH}. Thus, the relative contribution of T_{FH} and T_{FR} in the impairment in B cell selection during HIV infection remains to be determined.

In summary, we identified a population of macaque $CD4^+$ T cells with a phenotype, function, and location consistent with T_{FR}, and we revealed SIV-associated changes in the T_{FR}/T_{FH} ratio, adding to the complexity of humoral immunity to HIV.

Acknowledgments

We thank James Arthos and Claudia Cicala for helpful discussion, and Namal P. Liyanage, Dallas P. Brown, and Veronica Galli for critical reading of the manuscript.

Disclosures

The authors have no financial conflicts of interest.

References

1. Garside, P., E. Ingulli, R. R. Merica, J. G. Johnson, R. J. Noelle, and M. K. Jenkins. 1998. Visualization of specific B and T lymphocyte interactions in the lymph node. *Science* 281: 96–99.
2. Liu, Y. J., J. Zhang, P. J. Lane, E. Y. Chan, and I. C. MacLennan. 1991. Sites of specific B cell activation in primary and secondary responses to T cell-dependent and T cell-independent antigens. *Eur. J. Immunol.* 21: 2951–2962.
3. Jacob, J., G. Kelsoe, K. Rajewsky, and U. Weiss. 1991. Intraclonal generation of antibody mutants in germinal centres. *Nature* 354: 389–392.
4. Schwickert, T. A., G. D. Victora, D. R. Fooksman, A. O. Kamphorst, M. R. Mugnier, A. D. Gitlin, M. L. Dustin, and M. C. Nussenzweig. 2011. A dynamic T cell-limited checkpoint regulates affinity-dependent B cell entry into the germinal center. *J. Exp. Med.* 208: 1243–1252.
5. Kim, C. H., L. S. Rott, I. Clark-Lewis, D. J. Campbell, L. Wu, and E. C. Butcher. 2001. Subspecialization of $CXCR5^+$ T cells: B helper activity is focused in a germinal center-localized subset of $CXCR5^+$ T cells. *J. Exp. Med.* 193: 1373–1381.
6. Ansel, K. M., L. J. McHeyzer-Williams, V. N. Ngo, M. G. McHeyzer-Williams, and J. G. Cyster. 1999. In vivo-activated CD4 T cells upregulate CXC chemokine receptor 5 and reprogram their response to lymphoid chemokines. *J. Exp. Med.* 190: 1123–1134.
7. Schaerli, P., K. Willimann, A. B. Lang, M. Lipp, P. Loetscher, and B. Moser. 2000. CXC chemokine receptor 5 expression defines follicular homing T cells with B cell helper function. *J. Exp. Med.* 192: 1553–1562.
8. Petrovas, C., T. Yamamoto, M. Y. Gerner, K. L. Boswell, K. Wloka, E. C. Smith, D. R. Ambrozak, N. G. Sandler, K. J. Timmer, X. Sun, et al. 2012. CD4 T follicular helper cell dynamics during SIV infection. *J. Clin. Invest.* 122: 3281–3294.
9. Hong, J. J., P. K. Amancha, K. A. Rogers, C. L. Courtney, C. Havenar-Daughton, S. Crotty, A. A. Ansari, and F. Villinger. 2014. Early lymphoid responses and germinal center formation correlate with lower viral load set points and better prognosis of simian immunodeficiency virus infection. *J. Immunol.* 193: 797–806.
10. Breitfeld, D., L. Ohl, E. Kremmer, J. Ellwart, F. Sallusto, M. Lipp, and R. Förster. 2000. Follicular B helper T cells express CXC chemokine receptor 5, localize to B cell follicles, and support immunoglobulin production. *J. Exp. Med.* 192: 1545–1552.
11. Crotty, S. 2011. Follicular helper CD4 T cells (T_{FH}). *Annu. Rev. Immunol.* 29: 621–663.
12. Johnston, R. J., A. C. Poholek, D. DiToro, I. Yusuf, D. Eto, B. Barnett, A. L. Dent, J. Craft, and S. Crotty. 2009. Bcl6 and Blimp-1 are reciprocal and antagonistic regulators of T follicular helper cell differentiation. *Science* 325: 1006–1010.
13. Nurieva, R. I., Y. Chung, G. J. Martinez, X. O. Yang, S. Tanaka, T. D. Matskevitch, Y. H. Wang, and C. Dong. 2009. Bcl6 mediates the development of T follicular helper cells. *Science* 325: 1001–1005.
14. Chtanova, T., S. G. Tangye, R. Newton, N. Frank, M. R. Hodge, M. S. Rolph, and C. R. Mackay. 2004. T follicular helper cells express a distinctive transcriptional profile, reflecting their role as non-Th1/Th2 effector cells that provide help for B cells. *J. Immunol.* 173: 68–78.
15. Vinuesa, C. G., M. A. Linterman, C. C. Goodnow, and K. L. Randall. 2010. T cells and follicular dendritic cells in germinal center B-cell formation and selection. *Immunol. Rev.* 237: 72–89.
16. Schmitt, N., J. Bustamante, L. Bourdery, S. E. Bentebibel, S. Boisson-Dupuis, F. Hamlin, M. V. Tran, D. Blankenship, V. Pascual, D. A. Savino, et al. 2013. IL-12 receptor β1 deficiency alters in vivo T follicular helper cell response in humans. *Blood* 121: 3375–3385.
17. Vinuesa, C. G., I. Sanz, and M. C. Cook. 2009. Dysregulation of germinal centres in autoimmune disease. *Nat. Rev. Immunol.* 9: 845–857.
18. Goodnow, C. C., C. G. Vinuesa, K. L. Randall, F. Mackay, and R. Brink. 2010. Control systems and decision making for antibody production. *Nat. Immunol.* 11: 681–688.
19. Pratama, A., and C. G. Vinuesa. 2014. Control of T_{FH} cell numbers: why and how? *Immunol. Cell Biol.* 92: 40–48.
20. de Vinuesa, C. G., M. C. Cook, J. Ball, M. Drew, Y. Sunners, M. Cascalho, M. Wabl, G. G. Klaus, and I. C. MacLennan. 2000. Germinal centers without T cells. *J. Exp. Med.* 191: 485–494.
21. Warnatz, K., L. Bossaller, U. Salzer, A. Skrabl-Baumgartner, W. Schwinger, M. van der Burg, J. J. van Dongen, M. Orlowska-Volk, R. Knoth, A. Durandy, et al. 2006. Human ICOS deficiency abrogates the germinal center reaction and provides a monogenic model for common variable immunodeficiency. *Blood* 107: 3045–3052.
22. King, C., S. G. Tangye, and C. R. Mackay. 2008. T follicular helper (T_{FH}) cells in normal and dysregulated immune responses. *Annu. Rev. Immunol.* 26: 741–766.
23. Park, H. J., D. H. Kim, S. H. Lim, W. J. Kim, J. Youn, Y. S. Choi, and J. M. Choi. 2014. Insights into the role of follicular helper T cells in autoimmunity. *Immune Netw.* 14: 21–29.
24. Linterman, M. A., R. J. Rigby, R. K. Wong, D. Yu, R. Brink, J. L. Cannons, P. L. Schwartzberg, M. C. Cook, G. D. Walters, and C. G. Vinuesa. 2009. Follicular helper T cells are required for systemic autoimmunity. *J. Exp. Med.* 206: 561–576.
25. Linterman, M. A., W. Pierson, S. K. Lee, A. Kallies, S. Kawamoto, T. F. Rayner, M. Srivastava, D. P. Divekar, L. Beaton, J. J. Hogan, et al. 2011. $Foxp3^+$ follicular regulatory T cells control the germinal center response. *Nat. Med.* 17: 975–982.
26. Chung, Y., S. Tanaka, F. Chu, R. I. Nurieva, G. J. Martinez, S. Rawal, Y. H. Wang, H. Lim, J. M. Reynolds, X. H. Zhou, et al. 2011. Follicular regulatory T cells expressing Foxp3 and Bcl-6 suppress germinal center reactions. *Nat. Med.* 17: 983–988.
27. Lim, H. W., P. Hillsamer, A. H. Banham, and C. H. Kim. 2005. Cutting edge: direct suppression of B cells by $CD4^+$ $CD25^+$ regulatory T cells. *J. Immunol.* 175: 4180–4183.
28. Lim, H. W., P. Hillsamer, and C. H. Kim. 2004. Regulatory T cells can migrate to follicles upon T cell activation and suppress GC-Th cells and GC-Th cell-driven B cell responses. *J. Clin. Invest.* 114: 1640–1649.
29. Alexander, C. M., L. T. Tygrett, A. W. Boyden, K. L. Wolniak, K. L. Legge, and T. J. Waldschmidt. 2011. T regulatory cells participate in the control of germinal centre reactions. *Immunology* 133: 452–468.
30. Oestreich, K. J., S. E. Mohn, and A. S. Weinmann. 2012. Molecular mechanisms that control the expression and activity of Bcl-6 in T_H1 cells to regulate flexibility with a T_{FH}-like gene profile. *Nat. Immunol.* 13: 405–411.
31. Vaeth, M., G. Müller, D. Stauss, L. Dietz, S. Klein-Hessling, E. Serfling, M. Lipp, I. Berberich, and F. Berberich-Siebelt. 2014. Follicular regulatory T cells control humoral autoimmunity via NFAT2-regulated CXCR5 expression. *J. Exp. Med.* 211: 545–561.
32. Wolniak, K. L., S. M. Shinall, and T. J. Waldschmidt. 2004. The germinal center response. *Crit. Rev. Immunol.* 24: 39–65.
33. Mqadmi, A., X. Zheng, and K. Yazdanbakhsh. 2005. $CD4^+CD25^+$ regulatory T cells control induction of autoimmune hemolytic anemia. *Blood* 105: 3746–3748.
34. Moir, S., A. Malaspina, K. M. Ogwaro, E. T. Donoghue, C. W. Hallahan, L. A. Ehler, S. Liu, J. Adelsberger, R. Lapointe, P. Hwu, et al. 2001. HIV-1 induces phenotypic and functional perturbations of B cells in chronically infected individuals. *Proc. Natl. Acad. Sci. USA* 98: 10362–10367.
35. De Milito, A., A. Nilsson, K. Titanji, R. Thorstensson, E. Reizenstein, M. Narita, S. Grutzmeier, A. Sönnerborg, and F. Chiodi. 2004. Mechanisms of hypergammaglobulinemia and impaired antigen-specific humoral immunity in HIV-1 infection. *Blood* 103: 2180–2186.

36. Lindqvist, M., J. van Lunzen, D. Z. Soghoian, B. D. Kuhl, S. Ranasinghe, G. Kranias, M. D. Flanders, S. Cutler, N. Yudanin, M. I. Muller, et al. 2012. Expansion of HIV-specific T follicular helper cells in chronic HIV infection. *J. Clin. Invest.* 122: 3271–3280.
37. Cubas, R. A., J. C. Mudd, A. L. Savoye, M. Perreau, J. van Grevenynghe, T. Metcalf, E. Connick, A. Meditz, G. J. Freeman, G. Abesada-Terk, Jr., et al. 2013. Inadequate T follicular cell help impairs B cell immunity during HIV infection. *Nat. Med.* 19: 494–499.
38. Hong, J. J., P. K. Amancha, K. Rogers, A. A. Ansari, and F. Villinger. 2012. Spatial alterations between $CD4^+$ T follicular helper, B, and $CD8^+$ T cells during simian immunodeficiency virus infection: T/B cell homeostasis, activation, and potential mechanism for viral escape. *J. Immunol.* 188: 3247–3256.
39. Locci, M., C. Havenar-Daughton, E. Landais, J. Wu, M. A. Kroenke, C. L. Arlehamn, L. F. Su, R. Cubas, M. M. Davis, A. Sette, et al; International AIDS Vaccine Initiative Protocol C Principal Investigators. 2013. Human circulating $PD\text{-}1^+CXCR3^-CXCR5^+$ memory Tfh cells are highly functional and correlate with broadly neutralizing HIV antibody responses. *Immunity* 39: 758–769.
40. Vaccari, M., B. F. Keele, S. E. Bosinger, M. N. Doster, Z. M. Ma, J. Pollara, A. Hryniewicz, G. Ferrari, Y. Guan, D. N. Forthal, et al. 2013. Protection afforded by an HIV vaccine candidate in macaques depends on the dose of SIVmac251 at challenge exposure. *J. Virol.* 87: 3538–3548.
41. Pegu, P., M. Vaccari, S. Gordon, B. F. Keele, M. Doster, Y. Guan, G. Ferrari, R. Pal, M. G. Ferrari, S. Whitney, et al. 2013. Antibodies with high avidity to the gp120 envelope protein in protection from simian immunodeficiency virus SIV_{mac251} acquisition in an immunization regimen that mimics the RV-144 Thai trial. *J. Virol.* 87: 1708–1719.
42. Cecchinato, V., E. Tryniszewska, Z. M. Ma, M. Vaccari, A. Boasso, W. P. Tsai, C. Petrovas, D. Fuchs, J. M. Heraud, D. Venzon, et al. 2008. Immune activation driven by CTLA-4 blockade augments viral replication at mucosal sites in simian immunodeficiency virus infection. *J. Immunol.* 180: 5439–5447.
43. De Vos, J., D. Hose, T. Rème, K. Tarte, J. Moreaux, K. Mahtouk, M. Jourdan, H. Goldschmidt, J. F. Rossi, F. W. Cremer, and B. Klein. 2006. Microarray-based understanding of normal and malignant plasma cells. *Immunol. Rev.* 210: 86–104.
44. Vaccari, M., A. Boasso, Z. M. Ma, V. Cecchinato, D. Venzon, M. N. Doster, W. P. Tsai, G. M. Shearer, D. Fuchs, B. K. Felber, et al. 2008. $CD4^+$ T-cell loss and delayed expression of modulators of immune responses at mucosal sites of vaccinated macaques following SIV_{mac251} infection. *Mucosal Immunol.* 1: 497–507.
45. Hofmann-Lehmann, R., R. K. Swenerton, V. Liska, C. M. Leutenegger, H. Lutz, H. M. McClure, and R. M. Ruprecht. 2000. Sensitive and robust one-tube real-time reverse transcriptase-polymerase chain reaction to quantify SIV RNA load: comparison of one- versus two-enzyme systems. *AIDS Res. Hum. Retroviruses* 16: 1247–1257.
46. Romano, J. W., K. G. Williams, R. N. Shurtliff, C. Ginocchio, and M. Kaplan. 1997. NASBA technology: isothermal RNA amplification in qualitative and quantitative diagnostics. *Immunol. Invest.* 26: 15–28.
47. Wollenberg, I., A. Agua-Doce, A. Hernández, C. Almeida, V. G. Oliveira, J. Faro, and L. Graca. 2011. Regulation of the germinal center reaction by $Foxp3^+$ follicular regulatory T cells. *J. Immunol.* 187: 4553–4560.
48. Sage, P. T., L. M. Francisco, C. V. Carman, and A. H. Sharpe. 2013. The receptor PD-1 controls follicular regulatory T cells in the lymph nodes and blood. *Nat. Immunol.* 14: 152–161.
49. Xu, H., X. Wang, A. A. Lackner, and R. S. Veazey. 2014. $PD\text{-}1^{HIGH}$ follicular CD4 T helper cell subsets residing in lymph node germinal centers correlate with B cell maturation and IgG production in rhesus macaques. *Front. Immunol.* 5: 85.
50. Li, M. O., and R. A. Flavell. 2008. TGF-β: a master of all T cell trades. *Cell* 134: 392–404.
51. Sanjabi, S., L. A. Zenewicz, M. Kamanaka, and R. A. Flavell. 2009. Anti-inflammatory and pro-inflammatory roles of TGF-β, IL-10, and IL-22 in immunity and autoimmunity. *Curr. Opin. Pharmacol.* 9: 447–453.
52. Arce, J., M. Levin, Q. Xie, J. Albanese, and H. Ratech. 2011. T-regulatory cells in lymph nodes: correlation with sex and HIV status. *Am. J. Clin. Pathol.* 136: 35–42.
53. León, B., J. E. Bradley, F. E. Lund, T. D. Randall, and A. Ballesteros-Tato. 2014. $FoxP3^+$ regulatory T cells promote influenza-specific Tfh responses by controlling IL-2 availability. *Nat. Commun.* 5: 3495.
54. Moreno-Fernandez, M. E., W. Zapata, J. T. Blackard, G. Franchini, and C. A. Chougnet. 2009. Human regulatory T cells are targets for human immunodeficiency virus (HIV) infection, and their susceptibility differs depending on the HIV type 1 strain. *J. Virol.* 83: 12925–12933.
55. Li, S., E. J. Gowans, C. Chougnet, M. Plebanski, and U. Dittmer. 2008. Natural regulatory T cells and persistent viral infection. *J. Virol.* 82: 21–30.
56. Tran, T. A., M. G. de Goër de Herve, H. Hendel-Chavez, B. Dembele, E. Le Névot, K. Abbed, C. Pallier, C. Goujard, J. Gasnault, J. F. Delfraissy, et al. 2008. Resting regulatory CD4 T cells: a site of HIV persistence in patients on long-term effective antiretroviral therapy. *PLoS One* 3: e3305.
57. Grant, C., U. Oh, K. Fugo, N. Takenouchi, C. Griffith, K. Yao, T. E. Newhook, L. Ratner, and S. Jacobson. 2006. Foxp3 represses retroviral transcription by targeting both NF-κB and CREB pathways. *PLoS Pathog.* 2: e33.
58. Chevalier, M. F., and L. Weiss. 2013. The split personality of regulatory T cells in HIV infection. *Blood* 121: 29–37.
59. Boasso, A., M. Vaccari, A. Hryniewicz, D. Fuchs, J. Nacsa, V. Cecchinato, J. Andersson, G. Franchini, G. M. Shearer, and C. Chougnet. 2007. Regulatory T-cell markers, indoleamine 2,3-dioxygenase, and virus levels in spleen and gut during progressive simian immunodeficiency virus infection. *J. Virol.* 81: 11593–11603.
60. Cicala, C., J. Arthos, N. Censoplano, C. Cruz, E. Chung, E. Martinelli, R. A. Lempicki, V. Natarajan, D. VanRyk, M. Daucher, and A. S. Fauci. 2006. HIV-1 gp120 induces NFAT nuclear translocation in resting $CD4^+$ T-cells. *Virology* 345: 105–114.
61. Rao, A., C. Luo, and P. G. Hogan. 1997. Transcription factors of the NFAT family: regulation and function. *Annu. Rev. Immunol.* 15: 707–747.
62. Boyden, A. W., K. L. Legge, and T. J. Waldschmidt. 2012. Pulmonary infection with influenza A virus induces site-specific germinal center and T follicular helper cell responses. *PLoS One* 7: e40733.
63. Hu, T. T., X. F. Song, Y. Lei, H. D. Hu, H. Ren, and P. Hu. 2014. Expansion of circulating T_{FH} cells and their associated molecules: involvement in the immune landscape in patients with chronic HBV infection. *Virol. J.* 11: 54.
64. Feng, J., L. Lu, C. Hua, L. Qin, P. Zhao, J. Wang, Y. Wang, W. Li, X. Shi, and Y. Jiang. 2011. High frequency of $CD4^+$ $CXCR5^+$ T_{FH} cells in patients with immune-active chronic hepatitis B. *PLoS One* 6: e21698.
65. Chowdhury, A., P. M. E. Del Rio, G. K. Tharp, R. P. Trible, R. R. Amara, A. Chahroudi, G. Reyes-Teran, S. E. Bosinger, and G. Silvestri. 2015. Decreased T follicular regulatory cell/T follicular helper cell (T_{FH}) in simian immunodeficiency virus–infected rhesus macaques may contribute to accumulation of T_{FH} in chronic infection. *J. Immunol.* 195: 3237–3247.